IOP Publishing Journal of Physics: Condensed Matter
J. Phys.: Condens. Matter **29** (2017) 015102 (6pp) doi:10.1088/0953-8984/29/1/015102

A stochastic micro-machine inspired by bacterial chemotaxis

Hossein Mohammadi[1], **Banafsheh Esckandariun**[1] **and Ali Najafi**[1,2]

[1] Department of Physics, University of Zanjan, Zanjan 45371-38791, Iran
[2] Department of Physics, Institute for Advanced Studies in Basic Sciences (IASBS), Zanjan 45137-66731, Iran

E-mail: najafi@iasbs.ac.ir

Received 4 July 2016, revised 8 October 2016
Accepted for publication 11 October 2016
Published 10 November 2016

Abstract

Inspired by bacterial chemotaxis, we propose and study the dynamics of a 3D hydrodynamical search-machine at micrometer scale. Chemotactic memory of the proposed system that is borrowed from bacteria, allows it to search the fluid medium and find the required target. As the motion in micron size length scale is dominated by random forces, we analyze the statistical properties of the model. Mean square displacements, orientational correlation functions and also the chemotactic index (CI) of the system are investigated in detail. Because of the chemotactic memory, the system shows superdiffusing displacements in all directions and the diffusion exponents are anisotropic for the directions along or perpendicular to a preferred direction given by the gradient of attractant molecules transmitted by the target.

Keywords: chemotaxis, swimming, bacterium

(Some figures may appear in colour only in the online journal)

1. Introduction

Construction of micro-machines with the ability of performing directed motion toward a specific target at micrometer length scales, attracts many interests in recent years [1–3]. Devising smart cargo carriers and drug delivery systems in cellular environments, constructing efficient mixers in microfluidic and cell motility experiments are among the potential applications of such molecular machines [4–6].

From the physical principles, the inertia-less condition and also the presence of thermal fluctuations arising from impacts of fluid molecules, are the most important challenges that limit possible proposals for the engineering of micrometer scale motors. This means that the motion in micron scale is totally dominated by viscous forces and inertia has no effect in the motion at all [7, 8], one should note that at daily life we always benefit the inertia to produce efficient movements. In addition to overcoming this hydrodynamic peculiarity, any efficient search machine needs a kind of memory to compare its current position with its position at the previous step(s) to find and navigate through correct route.

Chemotaxis is a mechanism that microscopic organisms use to detect the right way toward their targets [9–12]. In this article, we benefit from the chemotaxis and propose a functional molecular machine. The phenomenon of chemotaxis has inspired extensive research both due to its direct biological relevance [13–15] and also because of the practical needs for designing artificial nano-robots that can sense the direction [16]. Random walk, is the traditional mathematical tool that can describe the fluctuating trajectories of a chemotactic bacterium [17–22]. True mathematical description of chemotaxis in terms of random walk, requires knowledge about the amount of jumping displacements, rotations and their transition probabilities. So far, theoretical studies on random walk modeling for microorganisms, do not consider both the hydrodynamical details and the mechanism of chemotactic memory in a unified model. In this article, we aim to construct a model that takes into account the details of hydrodynamical displacements, mechanism of chemotaxis memory and also the physics of fluctuations. We first introduce the hydrodynamical details of the system, then define the memory mechanism and finally the statistical properties of the model will be studied using numerical calculations.

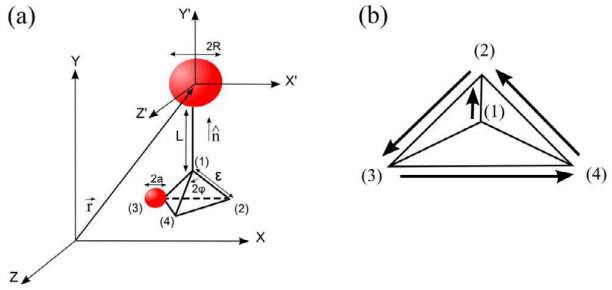

Figure 1. (a) A sphere with radius R models the body of a bacterium and a moving small sphere in resemblance with flagellum, provides the driving force. The hydrodynamical calculations are done in a co-moving frame of reference. (b) Amon all 12 possible internal transitions, we denote 4 of them as CW rotations. The rate of this CW rotations are determined by the chemotactic response function while the rate for other jumps are given randomly.

2. Hydrodynamical model

Our goal in this article is to combine the idea of chemical memory with a hydrodynamical model of a walker. Now let us introduce the hydrodynamical details of our system. Inspired by a bacterium, figure 1(a) shows the body of our walker that is modeled by a sphere of radius R. The driving force is modeled by a mobile small sphere with radius a. To simplify the mathematical details, we can assume that $a \ll R$. These two spheres are connected by an arm with negligible diameter. This model resembles the geometry of a bacterium with a single tail. As shown in this figure, and in a reference frame connected to the large sphere, jumps of this small sphere between 4 vertices of a pyramid will construct all internal discontinues jumps of our machine. The apex of this pyramid is a point with a distance L apart from the large sphere and is chosen as state (1). The other 3 states are located on the base of this pyramid. The apex angle is 2ϕ and the apex sides are ε. The base of this pyramid is an equilateral triangle with sides $2\varepsilon \sin\phi$. The angle φ may resemble the amplitude of flagellum undulations. The hydrodynamic question that we need to address here, is the differential change of the position and orientation of the system for an internal jump. For a fluid with viscosity η and at the condition of micron scale, the inertialess stokes equation $\eta\nabla^2\mathbf{u} - \nabla P = 0$, written for the fluid velocity $\mathbf{u}$ and pressure P, describes the dynamics. The condition of incomprehensibility, should also be considered. A prescribed motion corresponding to a jump of the small sphere, will enter to the dynamics through the boundary conditions. Solving the Stokes equation with the corresponding boundary conditions would result the dynamical properties of the large sphere during an internal jump. Calculations similar to the details presented elsewhere, reveals the dynamical results [23, 24]. To summarize the hydrodynamical results, let's denote the relative speed of small sphere with respect to the large sphere in each jump by v. Now the differential displacement and rotation of the large sphere in the laboratory frame for a jump from state (i) to state (j) read:

$$\Delta\vec{r}_{ij}^{\,H} = \mathcal{R}(\hat{n})\delta\vec{x}_{ij}, \quad \Delta\hat{n}_{ij}^{H} = \mathcal{R}(\hat{n})\delta\vec{\omega}_{ij} \times \hat{n},$$

where $\hat{n}$ represents the directer vector of the walker and $\mathcal{R}(\hat{n})$ is an appropriate rotation matrix that transform the co-moving frame of reference to the frame of laboratory. The co-moving frame is shown in figure 1(a). The differential rotations and displacements in the co-moving frame are given by:

$$\vec{\omega}_{12} = \begin{pmatrix} \frac{-2\alpha}{\sqrt{3}}\sin\varphi \\ 0 \\ -2\alpha\sin\varphi \end{pmatrix}, \quad \vec{\omega}_{24} = \begin{pmatrix} 3\alpha \\ 0 \\ \alpha \end{pmatrix}.$$

$$\delta\vec{x}_{12} = \begin{pmatrix} -\delta\sin\varphi \\ \delta' \\ \frac{\delta}{\sqrt{3}}\sin\varphi \end{pmatrix}, \quad \delta\vec{x}_{24} = \begin{pmatrix} \frac{\delta}{2} \\ 0 \\ \frac{-\sqrt{3}\,\delta}{2} \end{pmatrix},$$

where the parameters are defined as:

$$\alpha = \frac{3}{8}\left(\frac{\varepsilon}{R}\right)\left(\frac{a}{R}\right)\left(1+\frac{L}{R}\right), \quad \delta = \left(\frac{\varepsilon}{R}\right)\left(\frac{a}{R}\right)\left(1-\frac{3}{4}\frac{R}{L}\right),$$
$$\delta' = \left(\frac{\varepsilon}{R}\right)\left(\frac{a}{R}\right)\left(1-\frac{3}{2}\frac{R}{L}\right)\sqrt{1-\frac{4}{3}\sin^2\varphi}\,.$$

Please note that the results are presented for a walker with $\varepsilon \ll L$. The differential changes are given only for two jumps, a jump started from the apex and a jump in the base face of the pyramid. Other jumps can be obtained from these two special jumps by applying the appropriate rotation matrices. Symmetry requires that $\vec{\omega}_{ij} = -\vec{\omega}_{ji}$ and $\delta\vec{x}_{ij} = -\delta\vec{x}_{ji}$. A hydrodynamic time scale can be defined as: $\tau^H = \varepsilon/v$. This is the time for all the jumps that start from the apex of pyramid. The time for other jumps (all jumps in the base of pyramid) are given by: $2\tau^H \sin\varphi$.

General hydrodynamic arguments show that for an object with internal cyclic motions, a minimum number of two internal degrees of freedom, is necessary to achieve net propulsion at low Reynolds number (inertia-less) condition [7]. According to this so called Scalop theorem in low Reynolds hydrodynamics, Scalop (a system with one internal degree of freedom) is not able to swim. One should note that as our hydrodynamical system has a single internal degree of freedom (the distance between two spheres), there is no way to break the time reversal symmetry and achieve a finite propulsion during a full cycle of periodic motion. Any motion corresponding to a closed cycle along pyramid, will recover the initial state of the system.

In the next section we introduce the chemotactic memory of a bacterium then show how can we combine the idea of chemotactic memory with the above introduced hydrodynamical walker and construct a system with one internal degree of freedom that can move and find its target.

3. Chemotactic memory

To have a plan for internal jumps, we use the chemotactic strategy that bacteria use to navigate. Among different microorganisms, the chemical network responsible for chemotactic

signaling is well understood and studied in *Escherichia coli* [25–28]. Running state of this bacterium is due to the CCW (counter clockwise) rotation of flagella and changing the flagellar rotational state to CW (clockwise) will result a tumble. A set of chemical processes inside the cell provide a kind of chemical memory for the cell. These chemical signals, control the frequency of running and tumbling states. As a result of such memory, the organism can record a history of the food concentration along its trajectory. Depending on the conditions, a bacterium with this sort of memory will have chance to find a way to reach a point with maximum value of food concentration.

Now we want to combine the idea of chemotactic memory with the details of hydrodynamic jumps of the walker. Our modeling is based on stochastic jumps. Let denote the transition probability for jump from state (i) to state (j) by P_{ij}. In the case with $P_{ij} = 1/3$, we will have a random walker that has no chance to sense the direction of gradient. What we want to consider, is a sort of an intelligent walker that can dynamically change its jumping probabilities. In comparison with *E. coli*, we first define a set of jumps that corresponds to a CW rotation. We define all the following jumps as CW jumps:

$$CW \text{ jumps}: \quad 1 \to 2,\ 2 \to 3,\ 3 \to 4,\ 4 \to 2.$$

Please note that this definition for the CW rotations is not unique and other choices can work as well. In figure 1(b), all these CW jumps, are shown. After defining CW rotations, we assume that the probability for any CW jump is given by a signal $S(\vec{r}, t)$ from a chemotactic memory, and other jumps are determined randomly so that:

$$P_{ij} = \begin{cases} S(\vec{r}, t), & \text{CW jumps} \\ \dfrac{1 - S(\vec{r}, t)}{2}, & \text{otherwise.} \end{cases} \quad (1)$$

Here $\vec{r}$, is the position of the walker at time t. Similar to the chemotaxis signaling network of *E. coli*, we assume that the signal S, is connected to the source c (the local concentrations of food) through an intermediate dimensionless memory function m as: $S(\vec{r}, t) = \xi/(1 + \exp[m(\vec{r}, t) - v_0 c(\vec{r})])$ [27]. The dynamics of memory function is given by: $\dot{m}(\vec{r}, t) = (\tau^H/\tau_{ch})(S(\vec{r}, t) - \xi/3)$, where the dimensionless time scale of the adaptation is given by τ_{ch}/τ^H and v_0 is a constant that has the dimension of volume. For a uniform profile of the concentration, this system reaches a steady state with $S^*(\vec{r}, t) = \xi/3$. Here ξ is a parameter in the interval [0,1] and it shows how the internal jumps of the walker is anisotropic in the absence of any food gradient. Throughout this paper we will choose $\xi = 0.95$. For a nonuniform concentration profile, there is no static steady state solution and the system evolves in time by continuously adjusting its relative position and orientation with respect to the concentration profile.

To have more insights on the concept of memory time, we can introduce a quantitative measure for it. How much time does the system need to reach its equilibrium value $S = \xi/3$, when we make a sudden change in the concentration profile? This time would be a good choice for memory time. In figure 2, we have studied the response of the above chemical system

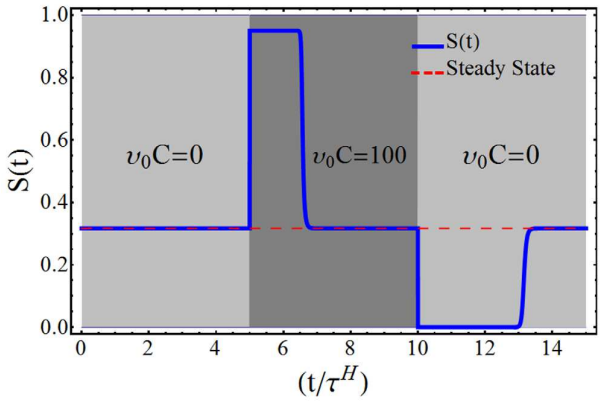

Figure 2. To study the dose-response curve of our system, the signal function $S(t)$, is plotted as a function of time. The concentration strength suddenly tune from zero to $v_0C = 100$ at time $t/\tau^H = 5$ and it turned off at time $t/\tau^H = 10$. Memory time is the time that system needs to reach its stationary state ($S = 1/3$), after a sudden change in concentration profile. Here $\tau_{ch}/\tau^H = 100$.

to a sudden change in concentration. For time in the interval $0 < t/\tau^H < 5$, the concentration is given by $v_0c = 0$ and the system is in its stationary state. On $t/\tau^H = 5$, we suddenly change the concentration profile to $v_0c = 100$ and keep it on till $t/\tau^H = 10$ then suddenly turn it off. As one can see, after any change in concentration, the signal function $S(t)$ will start to deviate from its stationary value. The memory time is the time that this deviation persists before reaching steady state. As it is evident from figure 2, the memory time shows different values when we turn the gradient on or off. This simple example shows that, the exact memory time, in principle is a complicated function of the different parameters of the system. The width of first non stationary plateau ($t = 5$ to 7) is smaller than the second plateau ($t = 10$ to 13). By plateau we mean a time interval that the signal S is different from its stationary value. This means that the chemical response time (memory time) for the cases when system feels an increase or a decrease in concentration are different. The memory time for a process with increasing food is much longer and for $0 < \tau_{ch}/\tau^H < 1$, the system can remember only the direction of food reduction and it will move toward the points with less food.

Throughout this paper, and for nonuniform food concentration, we choose a linear gradient field of the food concentration given by $c(x) = c_0 + \alpha x$. In non-dimensional units, the slope is given by:

$$\alpha = R|\nabla(v_0 c)|.$$

The statistical properties of this swimmer will be studied in details in the next section.

4. Results and discussions

We use a Monte Carlo like algorithm to simulate the dynamics of the walker. We put the walker at the origin with orientation along x-direction and choose a random internal stale for it then, try to generate its stochastic trajectory in space. As the

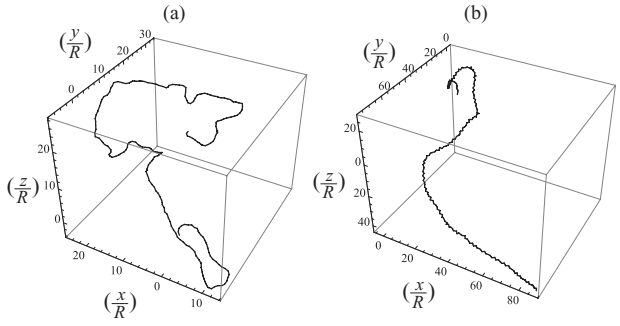

Figure 3. Two different trajectories for the walker are shown. Part (a) corresponds to a walker moving in a uniform concentration and (b) a linear concentration. Other numerical parameters are: $a = 0.2R$, $L = 6.1R$, $\varepsilon = 0.6R$, $\varphi = \pi/6$, $\tau^H = 0.02$, $\tau_{ch} = 100\tau^H$, $\alpha = 100$.

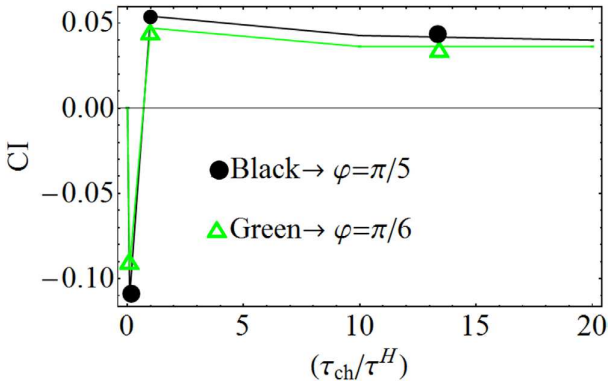

Figure 4. Chemotactic index in terms of the memory time is investigated for two walkers with different geometrical values. The positive result of the chemotactic mechanism is not sensitive to the geometrical parameter.

system move in discrete jumps, its trajectory is also discrete. Let us assume that in step i, the walker is located in position x_i, its orientation given by $\mathbf{n}_i$ and its internal state is given by α_i. For example if the state $\alpha_i = 1$, then three jumps $1 \to 2$, $1 \to 3$ and $1 \to 4$ are possible. Now to find its next state, using a random number routine, we generate a uniformly distributed random number in the interval [0,1]. As for any initial state α_i, there are three possible states, we divide the interval [1,0] into three distinct intervals [0,A], [A,B], [B,1]. We assume that, if the chosen random number belongs to the first interval ([0,A]) then the walker performs the jump: $1 \to 2$. If the random number lies in the interval [A,B] then the walker performs the jump $1 \to 3$ and finally if the random number lies in the third interval the walker perform the third transition. This is similar to Monte Carlo algorithm for simulating stochastic systems. Corresponding to each internal transition, we have their hydrodynamic movements that are given analytically in hydrodynamic section. Using the hydrodynamic movements, we can now calculate the new position and orientation of the walker. In this scheme, the most important part is the method with which we determine the numbers A and B. The length of the intervals should be proportional to the corresponding transition probabilities. For example, in the special example that we are using here, we choose $P_{12} = A$, $P_{13} = (B - A)$, $P_{14} = (1 - B)$. Using similar rules all internal jumps can happen with their appropriate probabilities.

Figure 3(a) shows a typical trajectory of the walker in a uniform concentration profile of food molecules. It represents the trajectory of a random walker. Typical trajectories for the walker moving in this concentration field is shown in figures 3(a) and (b), where the concentration is either uniform or nonuniform. As one can see, the subsequent tumbles bias the trajectory toward the place with larger concentration of food molecules. In the literature of chemotaxis, *CI* the chemotactic index is an important quantity that shows how accurate is a direction sensing mechanism [29]. It is defined as the ratio of the walking displacement along the concentration gradient to the total length of the walking trajectory. Depending on the dynamical variables of the system, *CI* belongs to the interval [−1,1]. In figure 4, *CI* is plotted in terms of the dimensionless memory time τ_{ch}/τ^H. Here τ_{ch} is a parameter that comes from the chemical dynamics and τ^H is a geometrical parameter. For large memory times ($\tau_{ch} \gtrsim \tau^H$), the chemotactic index is positive. This is a signature saying that the chemotactic mechanism has a positive result and the walker can successfully reach the target, the place of more food. As we discussed before, the chemotactic index for $0 < \tau_{ch}/\tau^H < 1$ is negative, denoting the fact that the system goes to region with less food.

As the time scale for a single jump is given by τ^H, this proves that τ_{ch} plays the role of a memory time. The memory time should be greater than the individual jumping time and this is the only condition required to have a successful gradient sensing walker.

The *CI* is calculated for two different values of the apex angle. It is seen that the result of the searching mechanism is not so sensitive to this angle. Now we can study the statistical properties of the system for $\tau_{ch} \gtrsim \tau^H$. One should note that due to small undulations approximation in our model, *CI* is very small and not comparable to real *E. coli*. To have a better understanding of the role of fluctuations, we repeat the simulations for an ensemble of walkers and have studied the average statistical properties of the system. Mean displacement (MD), mean square displacements (MSD) and correlation functions are the statistical variables that we consider. To quantify the results of MSD, we define the diffusion exponents as:

$$\langle x^2\rangle - \langle x\rangle^2 \sim t^{\nu_\parallel}, \quad \langle y^2\rangle - \langle y\rangle^2 = \langle z^2\rangle - \langle z\rangle^2 \sim t^{\nu_\perp},$$

where $\nu_\parallel$ and $\nu_\perp$ are the diffusion exponents along the gradient and along a direction perpendicular to the gradient, respectively. For a symmetric and normal random walker we have: $\nu_\parallel = \nu_\perp = 1$. MD for a random walker moving in uniform and nonuniform concentration profiles are presented in figure 5(a). As we expect, for uniform concentration the characteristics of a random walker is recovered, but for a nonuniform concentration with a gradient in x direction, the walker is biased toward the positive x direction. For nonuniform concentration, MD in the perpendicular directions ($\langle y\rangle$, $\langle z\rangle$)are zero but it is not zero in the direction of gradient ($\langle x\rangle$).

MSD in terms of time, in logarithmic scale, shows a nonlinear crossover from a short time to long time behavior. Figures 5(b) and (c) show the short and long time MSD results

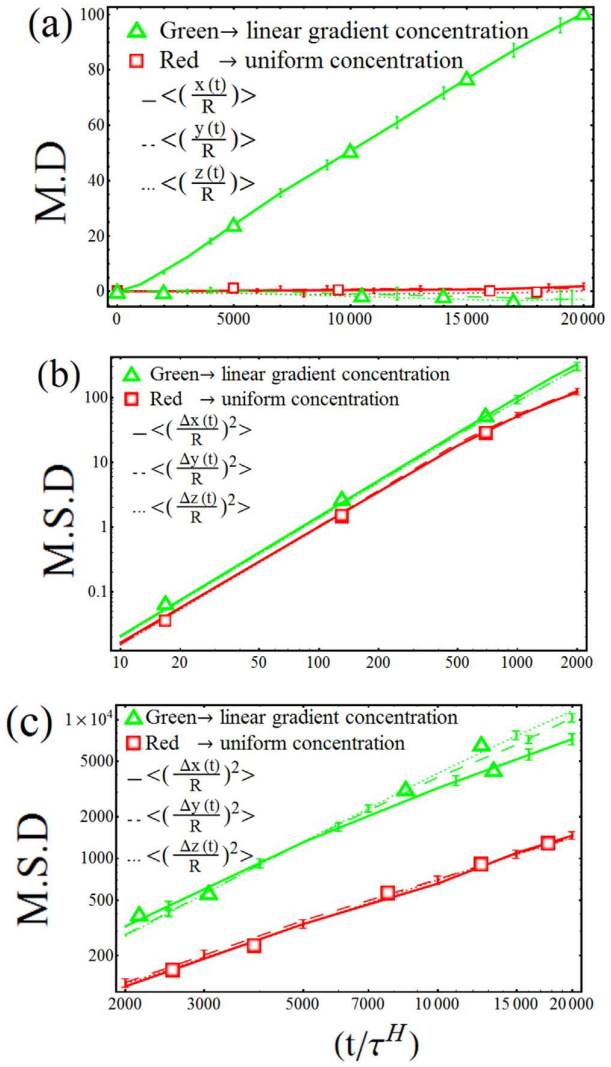

Figure 5. Statistical properties of walkers moving in either a uniform concentration or a concentration with a linear gradient. Part (a) shows average position of the walker as a function of time. As one can see a concentration with gradient in the x direction will result an average swimming to the positions with higher concentration of food. (b) shows the short time behavior of mean square displacement in terms of time and (c) shows the corresponding behavior at large time scales. The chemotaxis memory shows positive results only at large time scales. For a walker moving in uniform concentration, the long time and short time behaviors are separated by a nonlinear crossover. This reflects the non symmetric nature of our passive walker. The numerical parameters are as in figure 3 and $\alpha = 100$.

for this walker. This crossover is a result of the hydrodynamical anisotropy of the system. Please note that our system, spherical body with a connected tail, is anisotropic. A similar crossover is recently observed for a diffusing object with boomerang geometry [30]. Short time behavior for a walker moving in a linear concentration corresponds to $\nu_{\parallel} \approx \nu_{\perp} \approx 1.7$. Long time behavior of the walker moving in a uniform concentration with $R|\nabla(v_0 c)| = 0$, shows $\nu_{\parallel} = \nu_{\perp} = 1.0$, that characterizes a normal random walker (figure 5(c)). For a walker moving in a nonuniform concentration with $\alpha = 100$, the exponents are

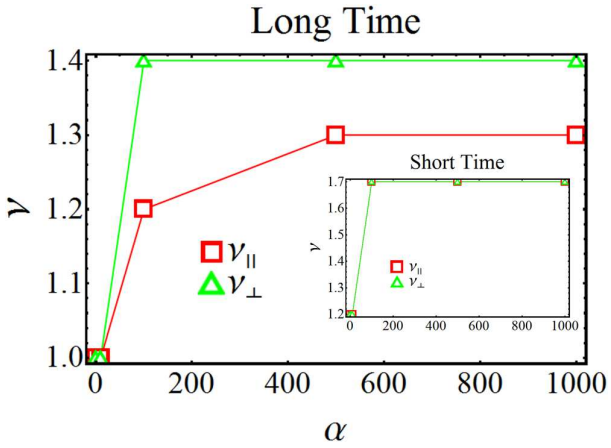

Figure 6. Long and short time behavior of diffusion exponents in terms of the concentration gradient. The numerical parameters are as in figure 3.

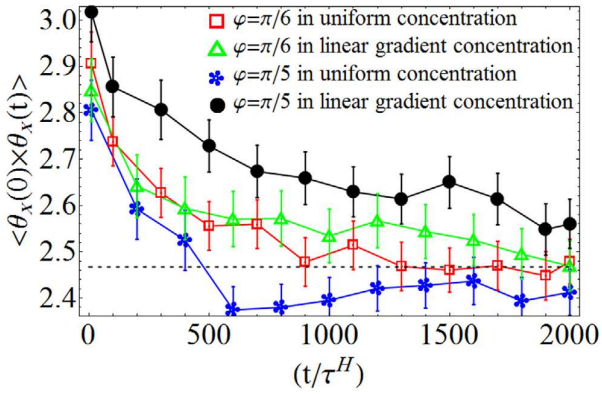

Figure 7. Orientational correlation function is plotted as a function of time. Here $\theta_x(t)$, is the angle that the director vector of walker makes with the x axis of the laboratory frame. Correlation time is sensitive on the geometrical variable (here φ) of the walker. For larger apex angle, the correlation function for a nonuniform gradient is larger than the corresponding value in uniform concentration. The dashed line shows the complete uncorrelated state with correlation $\pi^2/4$. The numerical parameters are as in figure 3.

given by $\nu_{\parallel} = 1.2$ and $\nu_{\perp} = 1.4$. The walker performs a super diffusion in all directions with an asymmetry in the direction parallel to the gradient concentration. Such a super diffusion motion in bacterial motion also has been observed [31]. In figure 6, we have studied the effects of the gradient strength on the diffusion exponents. As one can see, at larger gradient the diffusion exponents reach a constant values. To have more insights about the role of the geometry, we have studied the orientational correlation function $\langle\theta_x(0)\theta_x(t)\rangle$ where $\theta_x(t)$ represents the angle that the director of the walker makes with x axis (parallel to the concentration gradients). Figure 7, shows the features of the correlation function for walkers moving in uniform and nonuniform concentrations. Correlation time, the decay time for the correlation, is sensitive to the apex angle. For larger apex angles, the correlation time is also larger. This graph shows that the crossover time is essentially the time that orientational correlation washes out.

In conclusion, we have proposed a hydrodynamical micromachine and have studied its statistical properties in a gradient field produced by a target. Nontrivial coupling of geometrical parameters with dynamical characteristics, results interesting statistical properties of the machine. The memory time that is used in chemotactic mechanism, induces superdiffusion properties for the walker. A crossover from a short time to long time behavior of MSD is observed and the crossover time is the orientational correlation time. The hydrodynamic interaction between different walkers, is shown to have interesting features [32]. Along the extension of this work, we are considering the role of hydrodynamic couplings in the physics of interacting many walkers.

Acknowledgment

AN acknowledges the Abdus Salam international center for theoretical physics for hospitality during the final stage of this work.

References

[1] Kay E R, Leigh D A and Zerbetto F 2007 Synthetic molecular motors and mechanical machines *Angew. Chem., Int. Ed.* **46** 72–191
[2] Kinbara K and Aida T 2005 Toward intelligent molecular machines: directed motions of biological and artificial molecules and assemblies *Chem. Rev.* **105** 1377–400
[3] Willemsen J F 2010 Anomalous invasion in a 2D model of chemotactic predation *Physica* A **389** 3484–95
[4] Dittrich P S and Manz A 2006 Lab-on-a-chip: microfluidics in drug discovery *Nat. Rev. Drug Discovery* **5** 210–8
[5] Balzani V, Credi A, Raymo F M and Stoddart J F 2000 Artificial molecular machines *Angew. Chem., Int. Ed.* **39** 3348–91
[6] Irons C, Plank M J and Simpson M J 2016 Lattice-free models of directed cell motility *Physica* A **442** 110–21
[7] Purcell E M 1977 Life at low Reynolds number *Am. J. Phys.* **45** 3–11
[8] Huber G, Koehler S A and Yang J 2011 Micro-swimmers with hydrodynamic interactions *Math. Comput. Modelling* **53** 1518–26
[9] Berg H C 1975 Chemotaxis in bacteria *Annu. Rev. Biophys. Bioeng.* **4** 119–36
[10] Adler J 1966 Chemotaxis in bacteria *Science* **153** 708–16
[11] Van Haastert P J M and Devreotes P N 2004 Chemotaxis: signalling the way forward *Nat. Rev. Mol. Cell Biol.* **5** 626–34
[12] Kaupp U B, Kashikar N D and Weyand I 2008 Mechanisms of sperm chemotaxis *Annu. Rev. Physiol.* **70** 93–117
[13] Bray D 2001 *Cell Movements: From Molecules to Motility* (New York: Garland Science)
[14] Berg H C 2008 *E. coli in Motion* (Berlin: Springer)
[15] Friedrich B M and Jülicher F 2008 The stochastic dance of circling sperm cells: sperm chemotaxis in the plane *New J. Phys.* **10** 123025
[16] Dittrich P, Ziegler J C and Banzhaf W 2001 Artificial chemistries? A review *Artif. Life* **7** 225–75
[17] Codling E A, Plank M J and Benhamou S 2008 Random walk models in biology *J. R. Soc. Interface* **5** 813–34
[18] Berg H C 1993 *Random Walks in Biology* (Princeton, NJ: Princeton University Press) p 30
[19] Stevens A and Othmer H G 1997 Aggregation, blowup, and collapse: the ABC's of taxis in reinforced random walks *SIAM J. Appl. Math.* **57** 1044–81
[20] Lovely P S and Dahlquist F W 1975 Statistical measures of bacterial motility and chemotaxis *J. Theor. Biol.* **50** 477–96
[21] Hill N A and Häder D-P 1997 A biased random walk model for the trajectories of swimming micro-organisms *J. Theor. Biol.* **186** 503–26
[22] Howse J R, Jones R A L, Ryan A J, Gough T, Vafabakhsh R and Golestanian R 2007 Self-motile colloidal particles: from directed propulsion to random walk *Phys. Rev. Lett.* **99** 048102
[23] Najafi A and Zargar R 2010 Two-sphere low-Reynolds-number propeller *Phys. Rev.* E **81** 067301
[24] Najafi A 2011 Hydrodynamics of a microhunter: a chemotactic scenario *Phys. Rev.* E **83** 060902
[25] Bren A and Eisenbach M 2000 How signals are heard during bacterial chemotaxis: protein–protein interactions in sensory signal propagation *J. Bacteriol.* **182** 6865–73
[26] Falke J J, Bass R B, Butler S L, Chervitz S A and Danielson M A 1997 The two-component signaling pathway of bacterial chemotaxis: a molecular view of signal transduction by receptors, kinases, and adaptation enzymes *Annu. Rev. Cell Dev. Biol.* **13** 457
[27] Vladimirov N, Løvdok L, Lebiedz D and Sourjik V 2008 Dependence of bacterial chemotaxis on gradient shape and adaptation rate *PLoS Comput. Biol.* **4** e1000242
[28] Vladimirov N and Sourjik V 2009 Chemotaxis: how bacteria use memory *Biol. Chem.* **390** 1097–104
[29] Endres R G and Wingreen N S 2008 Accuracy of direct gradient sensing by single cells *Proc. Natl Acad. Sci.* **105** 15749–54
[30] Chakrabarty A, Konya A, Wang F, Selinger J V, Sun K and Wei Q-H 2013 Brownian motion of boomerang colloidal particles *Phys. Rev. Lett.* **111** 160603
[31] Taktikos J, Stark H and Zaburdaev V 2013 How the motility pattern of bacteria affects their dispersal and chemotaxis *PloS One* **8** e81936
[32] Najafi A and Golestanian R 2010 Coherent hydrodynamic coupling for stochastic swimmers *Europhys. Lett.* **90** 68003